Global analysis of thermal and chemical denaturation using CheMelt: Thermodynamic dissection of highly thermostable *de novo* designed proteins

Vili Lampinen[‡1,2,3,4] ; Osvaldo Burastero[‡,5,6] ; Iara Plácido Guazzelli[1,2,3,4] ; Florian Vögele[5,6] ; Francisca Pinheiro[1,2,3,4]; Jan S. Nowak[1] ; Maria M. Garcia Alai[*5,6] ; Magnus Kjaergaard[*1,2,3,4]

1 Department of Molecular Biology and Genetics, Aarhus University, Aarhus, Denmark
2 Interdisciplinary Nanoscience Center (iNANO), Aarhus University, Aarhus, Denmark
3 The Danish Research Institute of Translational Neuroscience (DANDRITE), Aarhus University, Aarhus, Denmark
4 The Center for Proteins in Memory (PROMEMO), Aarhus University, Aarhus, Denmark
5 European Molecular Biology Laboratory Hamburg, Notkestrasse 85, 22607, Hamburg, Germany
6 Centre for Structural Systems Biology, Notkestrasse 85, 22607 Hamburg, Germany

‡ Equal contribution
* Corresponding authors: magnus@mbg.au.dk, maria.garcia@embl-hamburg.de

ABSTRACT

De novo protein design often produces thermostable proteins that denature above 100 °C, which complicates the analysis of their stability. Thermostable proteins can be unfolded by combined chemical and thermal denaturation followed by global analysis of multiple melting curves. Here, we have developed CheMelt, a new online tool for global analysis of unfolding data via an intuitive graphical user interface. We use nanoscale differential scanning fluorimetry followed by CheMelt data analysis to dissect the combined thermal and chemical denaturation of thirty-five *de novo* designed protein binders. Fifteen present sufficient fluorescence changes to extract thermodynamic parameters of unfolding. These *de novo* designed proteins have systematically lower ΔC_p and *m*-values than comparable natural proteins, which implies that they expose fewer hydrophobic residues upon unfolding. We show that a high thermostability of a designed protein does not necessarily imply a high equilibrium stability; and demonstrate the potential of CheMelt in dissecting thermodynamic properties for protein design and engineering.

KEYWORDS: protein stability, *de novo* protein design, protein unfolding, CheMelt, eSPC

Link to Supplementary Information

INTRODUCTION

De novo designed proteins often exhibit high thermostability with melting temperatures routinely exceeding the boiling point of water (Cao et al., 2022; Vázquez Torres et al., 2025, 2024; Zheng et al., 2025). Thermostability is attractive for many biotechnological applications and may enhance activity by preserving the folded structure (Pezeshgi Modarres, Mofrad, & Sanati-Nezhad, 2016). High thermal stability may even be used for rapid purification of designed proteins by heat lysis (Grene et al., 2025; Pinheiro et al., 2025). While thermostability seems to be a general feature of *de novo* designed proteins, its structural and thermodynamic origin is unclear.

Protein thermostability has been extensively studied in the context of evolutionary adaptations for extremely hot environments (Jaenicke & Böhm, 1998). Homologous proteins from meso- and thermophiles have been compared to reveal how evolution tunes thermodynamic parameters to achieve thermostability (Sandeep Kumar, Chung-Jung Tsai, & Nussinov*§□, 2001). Based on these studies, three models of unfolding have been identified, which can be illustrated in a plot of the free energy of unfolding, ΔG_u, as a function of temperature (Figure 1) (Nojima, Ikai, Oshima, & Noda, 1977). First, thermophilic proteins could simply be very stable and have a higher ΔG_u at all temperatures. Second, the stability maximum could be shifted to higher temperatures. This would imply that they are close to cold denaturation at moderate temperatures and are initially stabilized upon heating. Third, thermostable proteins may be less sensitive to temperature, which happens when the change in heat capacity upon unfolding (ΔC_p) is small (Lindorff-Larsen & Teilum, 2021). These mechanisms can work together, and surveys of thermophilic proteins indicate that all three mechanisms are used by naturally thermostable proteins (Razvi & Scholtz, 2006).

For protein engineering, thermodynamic parameters of folding need to be determined accurately and with high throughput. Differential scanning fluorimetry (DSF) allows parallel measurement of many samples using minimal protein, so-called nanoDSF, making it highly suited for this purpose (Magnusson et al., 2019; Pantoliano et al., 2001). In a DSF experiment, proteins are thermally denatured while the fluorescence emission of aromatic residues or an extrinsic dye is monitored (Magnusson et al., 2019; Pantoliano et al., 2001). DSF can be extended to thermostable proteins by inclusion of chaotropic denaturants, which lower ΔG_u linearly with denaturant concentration (Privalov, 1979). By recording thermal denaturation traces at different denaturant concentrations, ΔG_u can be extracted as a function of denaturant concentration and extrapolated to the absence of denaturant. In practice, individual melting curves are often underdetermined and parameters are more robustly extracted by a global fit of curves recorded at a wide range of denaturant concentrations (Hamborg et al., 2020). Multivariate analysis of 2D unfolding data remains challenging for many laboratories and would benefit from more accessible, standardized analytical tools.

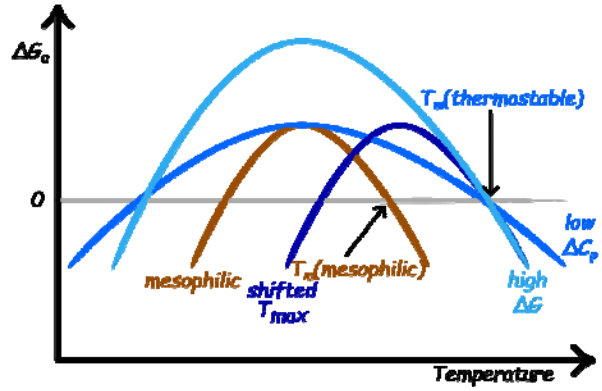

Figure 1. Hypothetical temperature profiles of free energies of unfolding of mesophilic and thermophilic proteins. The melting temperatures for denaturation are obtained from the points on the graph where ΔG_u=0. The melting temperature (T_m) of a protein can increase not only by shifting of an identically shaped curve (darkest blue), but also by an increase (light blue) or decrease (mid-blue) in maximum ΔG_u value, i.e. sharpening or flattening of the curve.

Here, we describe CheMelt, an online user-friendly tool for the global analysis of combined thermal and denaturant-induced unfolding. CheMelt is available at https://spc.embl-hamburg.de/app/chemelt, and is based on the Python package *pychemelt* (https://github.com/osvalB/pychemelt). Here, we first validated CheMelt with a previously published experimental dataset (Case I), then a dataset that simulates a highly thermostable protein (Case II), and finally, we use CheMelt to analyse nanoDSF data from fifteen highly thermostable *de novo* designed minibinders (Case III). We show that these designed proteins mainly achieve high thermostability via lower ΔC_p values than expected for proteins of their size.

RESULTS

SOFTWARE DESCRIPTION

We developed a new web tool called CheMelt for global analysis of denaturant and thermal denaturation. CheMelt is based on previous modules for the analysis of thermal unfolding data only: MoltenProt intended for fitting individual melting curves, and FoldAffinity intended for fitting ligand titration series (Burastero et al., 2021; Niebling et al., 2021). CheMelt is hosted together with a series of other tools for understanding of biophysical data at the eSPC platform (https://spc.embl-hamburg.de/).

The workflow of CheMelt can be conceptually divided into five steps (Figure 2). The first step allows import of files containing temperature, fluorescence intensities, and denaturant concentrations. The server natively supports output files from popular DSF instruments, e.g. Nanotemper Prometheus. In the second step, a fitting model is selected including equations

for how the baselines depend on temperature. The intercept and slope terms of the baselines can either be fitted globally (recommended) or individually for each curve. The third step is the actual fitting. For computational efficiency, it is possible to downscale the data density at this stage. The fourth step calls for an evaluation of the fit and parameter quality. Fits that give large and non-random residuals, or high error estimates should be critically re-evaluated. In the fifth step, it is possible to create publication quality figures as showcased in the figures of this manuscript. Practical instructions on how to use the server are detailed in the Supplementary Methods section (SI).

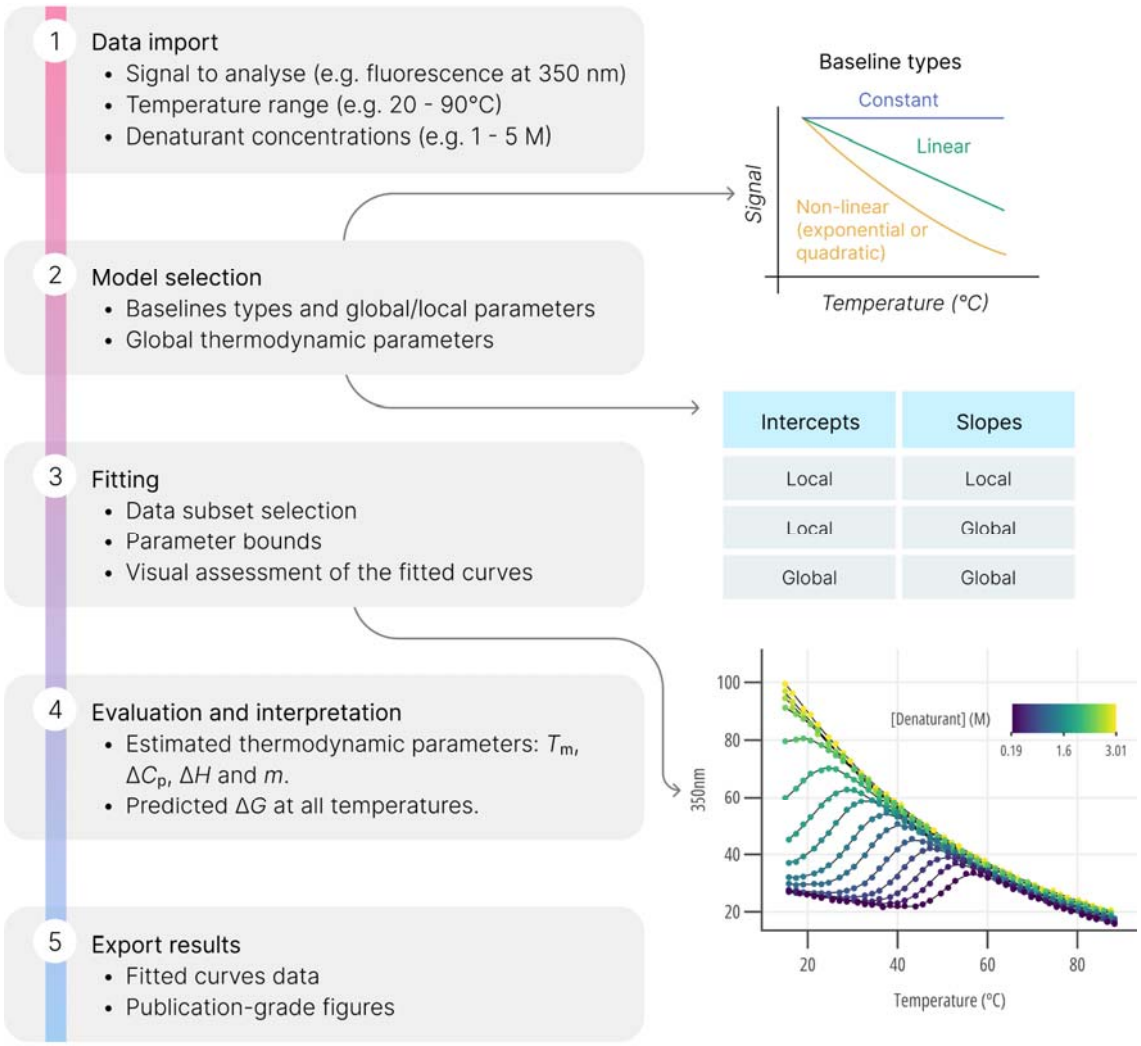

Figure 2. Workflow of CheMelt. 1) Data import, 2) Model selection, including the type of baselines, 3) Global fitting to estimate ΔC_p, T_m, ΔH and m, 4) Interpretation, and 5) Export of the results.

CASE I - ALGORITHM VALIDATION USING ACBP EXPERIMENTAL DATA

To test CheMelt, we reanalysed a dataset from bovine Acetyl-CoA binding protein (ACBP), a small helical bundle that has been used as a model system for protein folding studies (Teilum, Maki, Kragelund, Poulsen, & Roder, 2002; Thomsen, Kragelund, Teilum, Knudsen, & Poulsen, 2002). ACBP was used as a test case for combined denaturant and thermal unfolding resulting in a high quality data set (Hamborg et al., 2020). Previously, the temperature dependence for the native and unfolded states baselines were modelled with a linear and quadratic equation, respectively. However, we found that using an exponential equation for the unfolded baseline improved generalizability by deviating less from a completely unfolded curve after fitting (Figure S1). Subsequently, an exponential model for the unfolded baseline was used in this analysis. CheMelt derived global thermodynamic parameters, slopes and baselines fit the data well (Figure S2).

The fitted parameters strongly match the ones previously reported by Hamborg *et al.* (Hamborg et al., 2020). Especially, the melting temperature (T_m), heat capacity change (ΔC_p), and denaturant dependence of the unfolding free energy (*m*-value) are highly consistent between the two analyses (Table S1). Additionally, both CheMelt and Hamborg *et al.* report *m*-values and free energy of unfolding values that are in close agreement with previous measurements by Teilum *et al.* (Hamborg et al., 2020; Teilum, Kragelund, & Poulsen, 2002). These results show that CheMelt can fit experimental protein melting data and reproduce previously reported thermodynamic parameters.

CASE II - SIMULATED DATA OF HYPER-STABLE PROTEINS

A key application for CheMelt is the thermodynamic analysis of highly thermostable proteins. In such data sets, the desired parameters in the absence of denaturant cannot be measured directly, but they rather need to be extrapolated from melting curves recorded at high denaturant concentrations. Before analysing experimental data, we wanted to test whether CheMelt is still able to accurately extract thermodynamic parameters under these conditions using synthetic data. We simulated and fitted unfolding curves with fixed values (similar to ACBP) of ΔH, ΔC_p, m, but with variable T_m values spanning from 100 to 140 °C (Figure S3). Our results indicate that, even if there is no visible unfolding transition for the protein without denaturant, it is still possible to estimate a T_m value, as well as the other thermodynamic parameters (Figure S3).

CASE III - HYPER-STABLE *DE NOVO* DESIGNED PROTEINS

To explain the origin of the high thermal stability of *de novo* designed proteins, we selected thirty-five protein binders designed using a combination of RFdiffusion (Watson et al., 2023) and proteinMPNN (Dauparas et al., 2022). Seventeen of these proteins were reported previously as putative binders of the GK-domain of PSD-95 and the ALFA tag (Pinheiro et al., 2025). The remaining eighteen were designed as binders against the disordered C-

terminus of GluN1 (Table S2). All proteins are predicted to form a compact structure (Figure 4) by AlphaFold2 with a predicted alignment error (pAE) < 6.2 (Jumper et al., 2021) (Table S3), and remain soluble after purification by heat lysis. Except for two proteins (G3A and G5B), all the proteins in our test set were single domain alpha-helical bundles with 96–221 (median 118) amino acid residues.

As expected, none of the binders showed any significant denaturation without the presence of a denaturant, even at temperatures exceeding 90 °C. To identify suitable concentrations of denaturant for unfolding, we acquired nanoDSF measurements for all thirty-five proteins at 0, 2, 4, and 6 M guanidine hydrochloride (GdmCl) (Figure 3). For many of the proteins, a shift in 350 nm/330 nm ratio signal was observed only at one denaturant concentration. Lower and higher concentrations followed the pre- or post-transition baselines suggesting that the protein remains either fully folded or unfolded during the thermal gradient. Surprisingly, twenty out of thirty-five of the tested proteins did not show any transition in either fluorescence intensity at 330 nm, 350 nm, or their ratio (Figure 3C). While all tested proteins have at least one fluorescent residue, the proteins that did show an unfolding transition had more total and buried aromatic residues than those that did not (Figure S4). To test whether these proteins fail to unfold, we measured the unfolding of five proteins with flat nanoDSF traces using far UV circular dichroism spectroscopy (CD). CD showed that two of the proteins were mostly denatured at 25 °C in 6 M GdmCl (Figure S5A), two at 95 °C in 6 M GdmCl, while G15A still retains some □-helix character after spending more than fifteen minutes at 95 °C in 6 M GdmCl (Figure S5B). These five proteins thus all unfold at high denaturant and temperature, but their unfolding does not result in an observable change in fluorescence emission. As the focus of this work is nanoDSF analysis, we did not characterise these proteins further.

For the fifteen proteins that showed an observable melting transition, we performed nanoDSF at eleven GdmCl concentrations (Figure 4). A4A was included in the titration as it seemed to show a small transition in the screening, but subsequently eliminated from further analysis. The concentration range was determined individually for each protein based on the initial screen. Thirteen out of fifteen proteins showed sigmoidal unfolding curves, with a clear post-transition baseline, suggesting that full unfolding was achieved. One protein (G4B) failed to fully unfold even at 95 °C in the presence of 6 M GdmCl. All proteins except for G5A, the only beta-sheet containing protein, showed a full refolding upon cooling (Figure S6, S7) justifying the use of a reversible folding model.

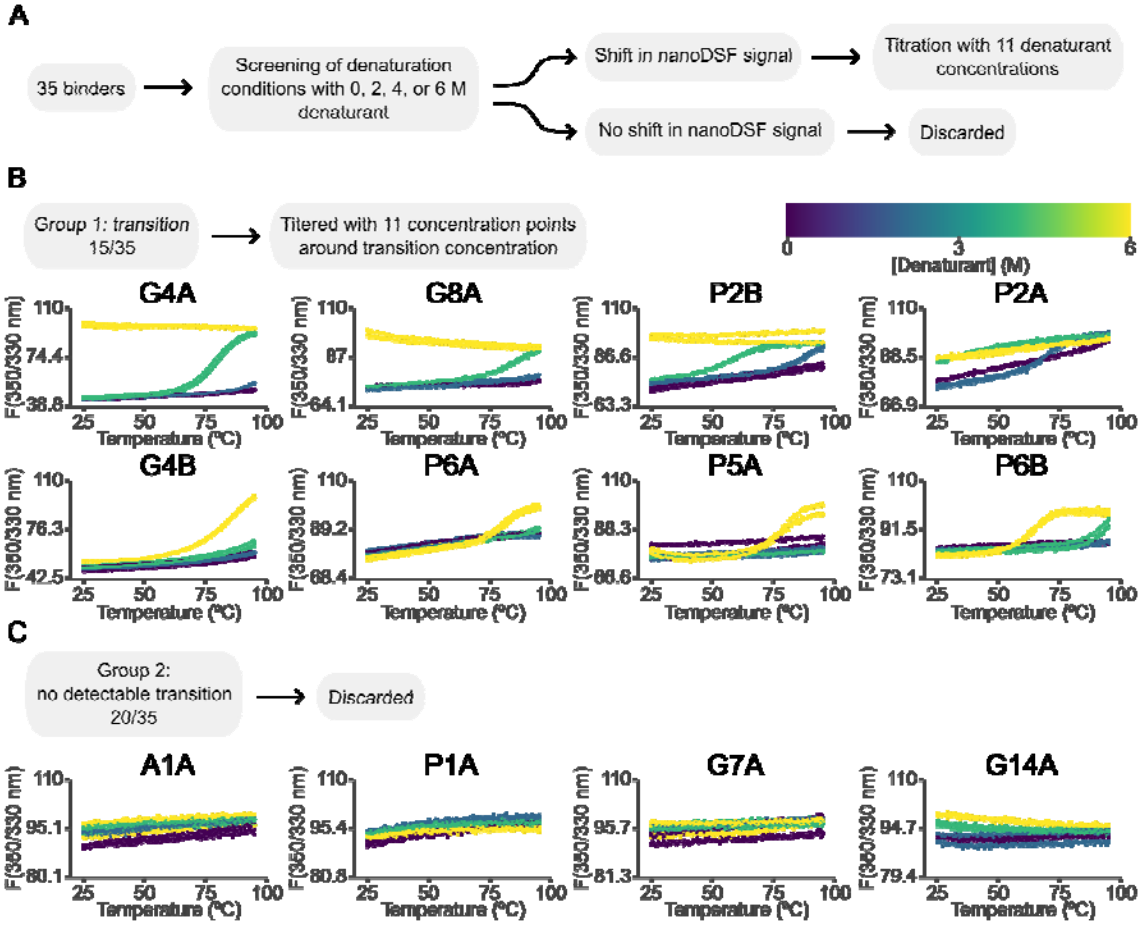

Figure 3. Screening of denaturation conditions for *de novo* designed protein binders. A) Flow chart of the screening process: *De novo* designed proteins were screened by nanoDSF at 0, 2, 4, and 6 M GdmCl to identify proteins with an observable unfolding transition. B) Representative melting curves of proteins that show an unfolding transition at least at one denaturant concentration. C) Representative DSF traces of proteins that do not show an unfolding transition. All graphs show two replicate measurements at each denaturant concentration and were prepared using the built-in tools in the CheMelt web server.

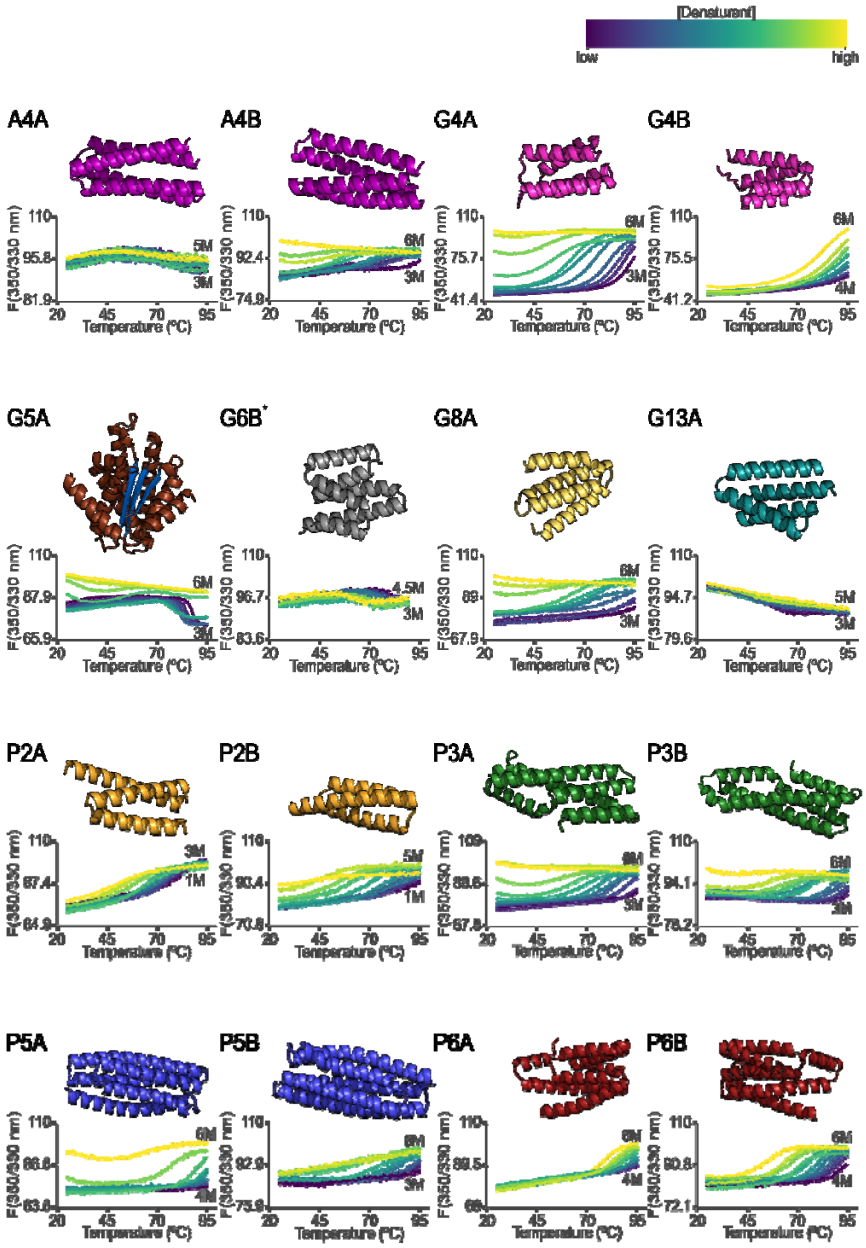

Figure 4. Combined thermal and denaturant titration of *de novo* designed proteins. Proteins with a detectable unfolding transition were titered in 0.2 or 0.3 M steps around the denaturant concentrations showing a transition in the screening. The highest (yellow) and lowest (purple) denaturant concentration is shown within each graph. Protein models represent an AlphaFold2 prediction above the corresponding melting curves and were prepared with PyMOL 3.1.1 (Schrödinger, LLC, 2024). Proteins with the same fold, but different sequences are shown with the same colors. A4A was included based on a minor shift during the screening, but was excluded from further analysis after the titration. For clarity, only a few concentrations are shown for protein G6B. All graphs were prepared using the built-in tools in CheMelt web server.

The ratio of fluorescence intensity (350 nm / 330 nm) is useful for visual inspection of melting curves; but it is not guaranteed to be proportional to the population of molecular species (Žoldák, Jancura, & Sedlák, 2017). Therefore, we used the raw fluorescence intensities for globally fitting all eleven melting curves for each protein (Figure 5). We used the 330 nm signal as it was most reproducible between repeats. The different appearances of the fluorescence traces necessitates different baseline models, so we tried progressively more complex baseline models for each protein until we found one that resulted in a good fit. The fit was regarded as successfully converging when the residuals were small, the relative error of the fitted parameters was less than 5%, and the thermodynamic parameters were plausible.

CheMelt produced robust fits to all fifteen proteins with thermodynamic parameters reported in Table I. As expected, all proteins were highly thermostable with melting temperatures near or above the boiling point of water (96 - 152 °C). The highest calculated melting temperature was 152 °C for G4B and the lowest 96 °C for P2A, with an average of 122 °C. In the end, we were able to fit all fifteen titered binders that showed a signal shift to the model, and generally, the fits matched the data closely (Figure 5).

Table I. Calculated thermodynamic parameters for the titered *de novo* binder proteins. The proteins are ranked by melting temperature, from highest to lowest T_m. The relative errors are calculated from the standard deviation of the fitted parameters.

		Values ± relative error (%)				
Rank	**Binder**	**T_m (°C)**	**T at ΔG_{max} (°C)**	**ΔH (kcal/mol)**	**ΔC_p (kcal/(mol×°C))**	***m* (kcal/(mol×M))**
1	G4B	152 ± 0.4%	40	75 ± 0.7%	0.58 ± 1.2%	1.5 ± 0.5%
2	P5A	143 ± 0.4%	47	96 ± 1.4%	0.88 ± 1.8%	1.7 ± 1.5%
3	G8A	135 ± 0.2%	38	113 ± 1.3%	1.02 ± 1.6%	2.6 ± 1.2%
4	P6B	134 ± 0.1%	32	122 ± 0.5%	1.04 ± 0.7%	2.4 ± 0.4%
5	P3B	133 ± 0.1%	32	75 ± 0.4%	0.65 ± 0.6%	1.7 ± 0.3%
6	P6A	128 ± 0.1%	37	90 ± 0.8%	0.88 ± 1.0%	1.6 ± 0.8%
7	P3A	127 ± 0.1%	34	84 ± 0.3%	0.80 ± 0.3%	2.0 ± 0.2%
8	G4A	122 ± 0.1%	30	94 ± 0.4%	0.90 ± 0.5%	2.2 ± 0.3%
9	A4B	121 ± 0.4%	7	43 ± 0.8%	0.32 ± 1.5%	1.1 ± 0.7%
10	P5B	116 ± 0.4%	26	88 ± 1.5%	0.86 ± 2.1%	2.3 ± 1.2%
11	P2B	113 ± 0.2%	17	63 ± 1.0%	0.57 ± 1.4%	1.7 ± 0.8%

12	G6B	112 ± 0.3%	39	116 ± 2.2%	1.43 ± 2.6%	2.3 ± 2.1%
13	G13A	100 ± 0.1%	9	61 ± 0.4%	0.58 ± 0.6%	1.7 ± 0.3%
14	G5A	96 ± 0.1%	56	155 ± 1.2%	3.65 ± 1.2%	1.2 ± 1.3%
15	P2A	96 ± 0.2%	25	65 ± 1.2%	0.83 ± 1.6%	1.9 ± 1.0%

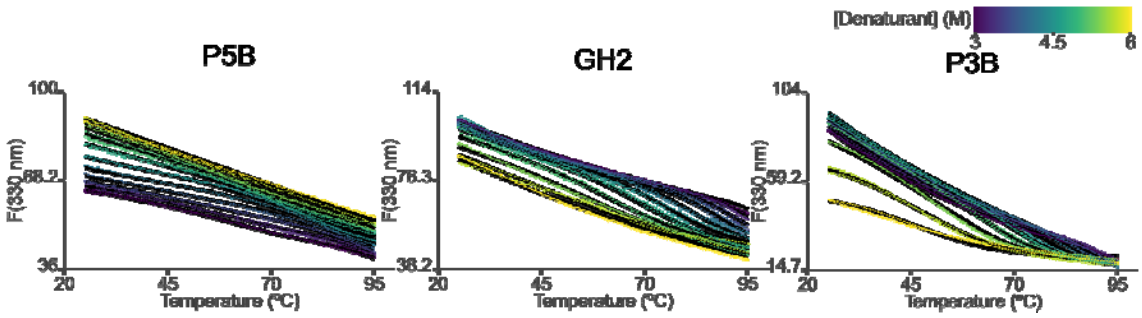

Figure 5. Fitting of denaturation data for *de novo* binder proteins. The model was fitted to the 330 nm fluorescence intensity signal for each titered protein. The figure shows three representative examples of binder denaturation curves normalised for signal intensity to improve clarity and prevent overlap. Scatter plots show the experimental data, with color coding indicating the GdmCl concentration with two replicate measurements for each. Solid black lines represent the global fits to the unfolding model at each denaturant concentration. All graphs were prepared using the built-in tools in CheMelt web server.

Protein unfolding leads to a change in the solvent accessible surface area (ΔSASA), which is tightly correlated to the heat capacity change upon unfolding (ΔC_p) and the dependence of the free energy on the denaturant concentration (*m*-value) (Myers, Pace, & Scholtz, 1995). As ΔSASA scales with protein chain length, both ΔC_p and *m*-values scale linearly with the number of residues, and the two parameters are highly correlated. We compared the ΔC_p and *m*-values from our present data set of *de novo* designed proteins with a dataset collected from natural single domain proteins from Myers *et al.* 1995 (Myers et al., 1995). The ΔC_p and *m*-values in our dataset exhibit a correlation and slope similar to those reported by Myers *et al.* indicating internal consistency of the data and suggesting that they reflect ΔSASA upon unfolding (Figure 6A). However, the correlation of ΔC_p and *m*-value with the number of residues showed a substantially lower slope than found by Myers *et al.* (Figure 6B–C). G5A is a notable outlier, being the only protein with a β-sheet fold and unable to refold upon cooling. β-sheet rich proteins are generally more difficult to design and express due to their reliance on non-local interactions (Marcos et al., 2018). While unfolding of β-sheet proteins such as immunoglobulin (Ig) domains can be reversible, many are irreversibly trapped in a denatured state (Rief, Gautel, Oesterhelt, Fernandez, & Gaub, 1997; Vermeer & Norde, 2000).

In the stability plots in Figure 1, ΔC_p determines the curvature as the second derivative of the free energy of folding with respect to the temperature. To assess how our *de novo* proteins behave relative to natural proteins, we compare stability plots derived from experimental parameters (ΔH, ΔC_p, and T_m) with hypothetical plot constructed using the ΔC_p value expected for a protein of the same length (Myers et al., 1995) (Figure 6D-F). The *de novo* designed proteins have a flattened stability plot, with the effect being most pronounced for larger proteins. Incidentally, small proteins always have a relatively low thermal sensitivity due to their small hydrophobic cores (Alexander, Fahnestock, Lee, Orban, & Bryan, 1992). In conclusion, the proteins in our data set primarily achieve their high thermostability through a reduced temperature sensitivity rather than a high equilibrium stability, as has been previously proposed for thermophilic proteins (Zhou, 2002).

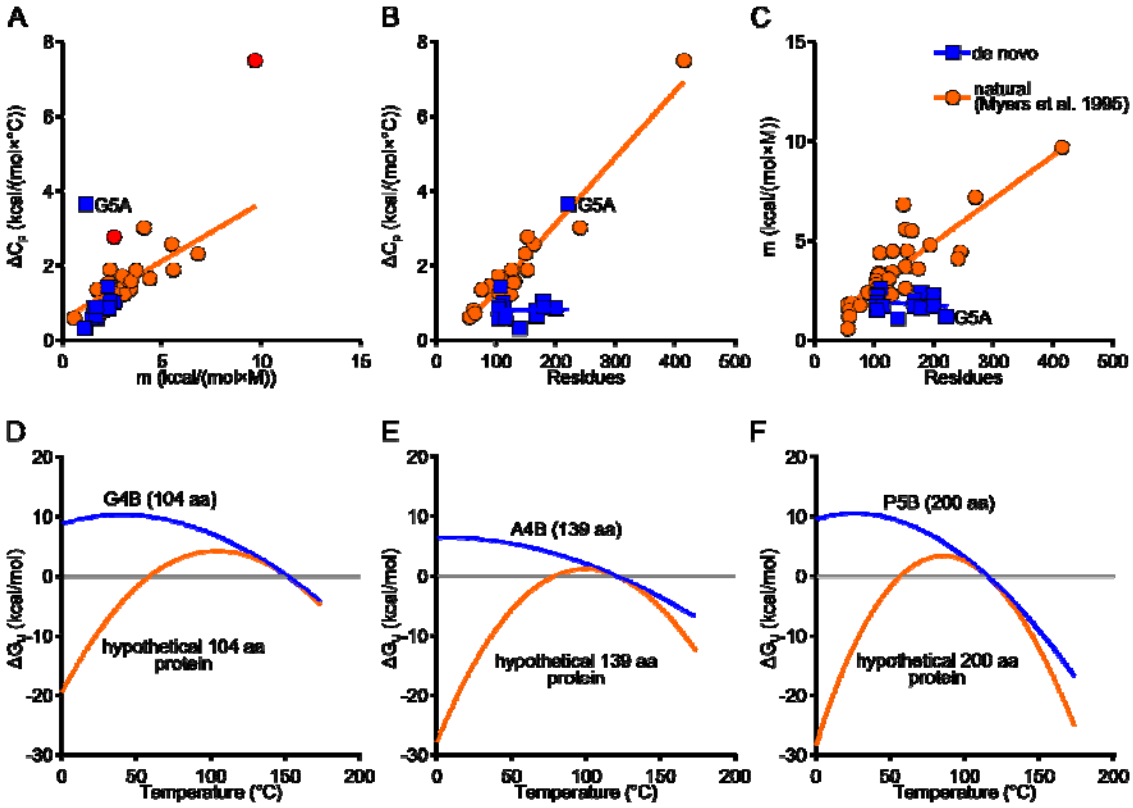

Figure 6. Comparison of thermodynamic parameters of *de novo* binders and native proteins. The list of native proteins and their thermodynamic parameters were extracted from Myers *et al.* 1995 (Myers et al., 1995). The lines show linear regression of the data, excluding binder G5A as an outlier in panel B. D–F) The stability plots of three example proteins from the study are compared with proteins with the same length, melting temperature and *ΔH* value but with a predicted ΔC_p value, instead of an experimentally determined one. The plots were prepared using GraphPad Prism 11.0.0. The predicted ΔC_p value was calculated as 0.0142 kcal/mol**n* + 0.0025 kcal/mol, where *n* is the number of residues (Myers et al., 1995).

DISCUSSION

We have developed CheMelt as a graphical user interface for global analysis of combined denaturant and thermal denaturation of proteins. By providing a user-friendly, web-based server, we aim to lower the barrier to entry and promote broader use of this methodology. The ability to determine thermodynamic parameters was similar to that reported by Hamborg *et al. (*Hamborg et al., 2020*).*

The rise of *de novo* protein design will increase the need for analysis of thermostable proteins. Nanoscale DSF is a convenient candidate for such studies, although many recent design papers have used CD spectroscopy to assess stability (e.g.(Cao et al., 2022; Koga et al., 2020; Vázquez Torres et al., 2025, 2024; Zheng et al., 2025)). Compared to CD, nanoDSF uses less material and is easier to run for many samples in parallel. A disadvantage is that not all proteins will have a detectable unfolding titration in the fluorescence emission. Here, we only observed an unfolding transition for 15 out of 35 (43%) of the proteins tested. Using CD spectroscopy, we showed that a selection of proteins without a fluorescence transition unfold with similar melting temperatures as the ones with a detectable transition. This suggests a minimal environmental change of the aromatic residues upon unfolding, pointing to a difference in the hydrophobic cores of the designed proteins. Our test set of designed proteins is dominated by small helical bundles, which do not leave much room for bulky tryptophan residues in the interior, especially in the idealized tight packing favored by machine learning algorithms. The lack of fluorescence changes may generalise to other helical mini-binders, but not necessarily to designed proteins with other folds.

Fitting of thermodynamic models to fluorescence-based unfolding data will often be an ill-posed problem, so a set of unfolding curves can be explained by different combinations of parameters. Compared to other experimental techniques, nanoDSF data is challenged by pre- and post-transition baselines that are often non-linear. Currently, the baselines are modelled empirically, although Zimm-Bragg theory (Seelig & Schönfeld, 2016) provides a conceptual foundation for curved baselines. Compared to melting curves for protein folding model systems (e.g. ACBP), the designed proteins tested here are more challenging to fit due to the combination of a small change in fluorescence parameters as discussed above, and a broad unfolding transition. The latter is a consequence of the low ΔC_p and shallow dependence of equilibrium constant on temperature discussed below. From a fitting perspective, this makes it more difficult to deconvolute the sloping baselines and the unfolding transition. Even under these challenging conditions, CheMelt converges to unique parameter sets for the fifteen proteins tested here. It should be noted, that the fitting routine is not guaranteed to work for all proteins, and especially prone to fail if the data set cannot uniquely constrain the baselines in at least one melting curve. For highly thermostable proteins, it should be ensured that the highest denaturant concentration reveals sufficient post-transition baseline before fitting.

We found that the ΔC_p value of unfolding of the *de novo* designed proteins is much lower than for natural proteins of a similar length. This finding does not necessarily generalize to all *de novo* designed proteins as a few caveats should be noted: The dataset used here are all mini-binders with exposed hydrophobic binding patches, and all have been designed with a similar workflow based on RFdiffusion (Watson et al., 2023) and proteinMPNN (Dauparas et al., 2022) followed by ranking by AlphaFold2 (Jumper et al., 2021). Similarly, the data set is almost exclusively composed of small □-helical bundles, and the only β-sheet containing protein was a noticeable outlier. Nevertheless, our results show that a low ΔC_p is one mechanism by which protein design algorithms can achieve thermostability, similar to what has been proposed for proteins from thermophilic organisms (Razvi & Scholtz, 2006).

Large positive ΔC_p values for protein folding are widely accepted to reflect the burial of hydrophobic groups, in analogy with the effect observed upon transfer of hydrocarbons to water (Baldwin, 1986; Spolar, Livingstone, & Record, 1992). This could be explained by the hydrophobic core of the designed proteins not being fully dehydrated, or having a higher degree of residual structure in the denatured state. In support of the former, mutation of the hydrophobic core of a hyperstable *de novo* designed protein to mainly contain valine residues resulted in a more dynamic hydrophobic core and a lower ΔC_p (Koga et al., 2020). Alternatively, it has been suggested that proteins from thermophiles rely more on polar interactions in the folded state and that this contributes to their low ΔC_p value (Zhou, 2002). Our present data set is likely not large enough nor general enough to deduce the origin of the effect.

High stability is often highlighted as an advantage of *de novo* designed proteins. In certain applications, thermal stability is an essential property, for example in industrial processes that occur at high temperatures. In other cases, high thermal stability may be viewed as a proxy for stability towards other types of perturbations. In the latter case, it is important to distinguish between high thermal stability achieved through a high ΔG_u, and through a low ΔC_p. A high ΔG_u implies a low fraction of the unfolded state at room temperature. Therefore, a high ΔG_u will likely also translate into robustness against undesirable reactions occurring via the unfolded state such as aggregation or proteolysis. High thermal stability achieved predominantly through a low ΔC_p does not imply a low fraction of unfolded state at room temperature. By extension, thermostability achieved through a low ΔC_p will likely not provide robustness against other challenges of the integrity of the protein. When characterising the stability of proteins in design and engineering, it is thus advisable to do a full characterisation of the thermodynamics parameters rather than relying on melting temperature as the sole metric for stability. CheMelt provides a robust data analysis platform for such characterisation.

MATERIALS AND METHODS

SIMULATED DATA

The Case I data was simulated using a linear baseline for the native state and an exponential baseline for the unfolded state.

EXPERIMENTAL DATA

ACBP fitting

The unfolding curves of ACBP were downloaded from Github (https://github.com/KULL-Centre/ProteinUnfolding2D/tree/main/examples/data)(Hamborg et al., 2020). The sixteen unfolding curves were measured between 15 and 95 °C, at different GdmCl concentrations up to 3 M in approximately 0.2 M steps. The zero molar denaturant concentration was excluded from the analysis. The signals at 330 nm and 350 nm were fitted simultaneously with *pychemelt*. A linear baseline was used for the native state and an exponential baseline for the unfolded state. The data were reduced to a subset of maximally 200 data points per curve prior to fitting. The model was fitted to the data with globally shared thermodynamic parameters, slopes and baselines. A scaling factor was applied to each concentration to correct for experimental variability.

Design and production of proteins

The *de novo* binder proteins (targeting ALFA-tag, GluN1 C terminal domain (CTD), PSD-95 GK-domain) were designed using RFDiffusion (Watson et al., 2023) and ProteinMPNN (Dauparas et al., 2022). The first letter of the name of each binder refers to the binding target, whereas the latter letter indicates different sequences with the same fold. A and P minibinders were reported previously. G minibinders (Table S2) were designed against a peptide (VLPRRAIEREEGQLQL) from GluN1 CTD and selected by a low $PAE_{interaction}$ as predicted by AlphaFold2, which also confidently predicts their monomeric structure (Table S3). The binders were ordered as synthetic genes from Twist Bioscience (USA), who also subcloned them into pET-28a(+) vectors using the NdeI/XhoI restriction sites, so all binders have a 6×His-tag followed by a thrombin site (GluN1 binder sequence Table S2). All binders were expressed in *E. coli*, heat-lysed at 95 °C and purified with Ni-NTA chromatography as previously described (Pinheiro et al., 2025). The proteins were flash-frozen and stored at -20 °C until analysis. All binders were more than 95% pure after the chromatography based on visual inspection of SDS-PAGE gels (Figure S8, other binders described earlier (Pinheiro et al., 2025)). Binders G5A, G14A, G10A, and G4A showed as double bands in the gel (with the smaller band assumed to be a product of proteasis of the binder), but they were still included in the screening stage, and G5A and G4A into titration.

Nanoscale differential scanning fluorimetry screening

Unfolding was initially screened for thirty-five binders based on their intrinsic fluorescence with nanoDSF (Prometheus Panta, Nanotemper, Germany). Each binder was measured at a

final concentration of 10 µM in the presence of 0, 2, 4, or 6 M GdmCl dissolved in phosphate-buffered saline (PBS, pH 7.4). Two replicates of each sample were prepared in 10 µL capillaries (Prometheus standard capillaries, Nanotemper, #PR-C002), and the capillaries were heated in the instrument from 25 to 95 °C, 4 degrees/min with no refolding observation or dynamic light scattering (DLS) measurement.

Nanoscale differential scanning fluorimetry titration

For GdmCl titration, two replicate samples of the binders were prepared as described above with eleven GdmCl concentrations around the concentration showing a transition in the screening. We titered all sixteen binder hits in five different concentration groups with increment increases of 0.2 or 0.3 M GdmCl that span a range of 2 or 3 M change in concentration. In the titration unfolding measurement, the temperature was increased one degree/min from 25 to 95 °C and cooled back to 25 °C at the same rate to measure refolding.

Fitting of nanoDSF data of *de novo* designed proteins

NanoDSF data was transferred into CheMelt by exporting the unfolding curves as a raw data Excel file using the Nanotemper Panta Analysis software. The 330 nm fluorescence intensity was fitted to a two-state unfolding model as described above for ACBP data, except that we did not reduce the data density. Different baseline signal dependence settings were tested until the errors of the fitted thermodynamic parameters were less than 5 %.

Circular dichroism spectroscopy (CD)

Five *de novo* designed proteins (G12A, A1A, G10B, A1B, and G15A) that did not show a fluorescence shift were studied by circular dichroism (CD). We measured the CD spectra on a Jasco-810 spectropolarimeter (Jasco, Tokyo, Japan) at 25 °C using a thermoelectric temperature controller (Jasco-PTC-348W1). The CD measurements were made in a 1 mm quartz cuvette using wavelengths between 190 and 260 nm with a data pitch of 1 nm, scanning speed of 50 nm/min and a 1 nm bandwidth. For some CD measurements, we did only two measurements and show a representative one, for others, we show averages of three replicates. All CD spectra were background corrected by subtracting the signal of the relevant buffer. We truncated the spectra to start at 212 nm to cut out the part where the high-tension voltage on the photomultiplier tube exceeds 650 V due to GdmCl signal. The data was analysed using the ChiraKit web tool (Burastero et al., 2025).

THEORY

COMBINED CHEMICAL AND THERMAL DENATURATION

The combination of both denaturation methods results in the following expression for the free energy of unfolding (See Supplementary Methods section, SI):

$$\Delta G(T, C) = \Delta H\left(1 - \frac{T}{T_m}\right) + \Delta C_p\left(T - T_m - T\ln\left(\frac{T}{T_m}\right)\right) - m \cdot C$$

where T is the temperature in Kelvin units, D is the denaturant concentration in molar units, ΔH is the enthalpy of unfolding, T_m is the temperature of melting, ΔC_p is the heat capacity of unfolding, and m is an empirical parameter that allows modelling ΔG with a linear dependence on denaturant concentration (Greene & Pace, 1974). The fraction of protein in the folded (f_n) and unfolded (f_u) states is then calculated as:

$$f_n(T) = \left(1 + e^{-\frac{\Delta G(T,D)}{RT}}\right)^{-1}$$
$$f_u(T) = 1 - f_n$$

where R is the gas constant.

FITTING EQUATION

The total signal is assumed to be a linear combination of the signal produced by the different protein states weighted by their mole fractions.

$$S(T, D) = f_n(T, D) \cdot S_n(T, D) + f_u(T, D) \cdot S_u(T, D)$$

where $S_n(T, D)$ and $S_u(T, D)$ are functions describing the signal dependence on temperature and denaturant concentration for the native and unfolded states, respectively. The dependence on temperature can be modelled with a constant, linear, quadratic, or exponential equation (See Supplementary Methods section, SI). Each denaturation curve can have local or shared baseline parameters.

The baseline dependence on denaturant concentration is only considered if the intercepts terms are shared (See Figure 1). In that case, it is assumed to be linear, and a scaling term, for each denaturation curve, can be included in the fitting.

ASSUMPTIONS OF THE FITTING MODEL

The fitting model used by CheMelt rests on several assumptions: The protein under study must be a monomer, the unfolding should follow a reversible two-state process. The heat capacity of unfolding ΔC_p and m-value are considered to be independent from temperature and denaturant concentration. Then, the background signal must be negligible (or constant) and that the folded and unfolded states produce a different signal. In this regard, the ensemble of thermally-induced and denaturant-induced unfolded states are considered to be equal. Furthermore, the denaturant contribution to the free energy of unfolding for chemical denaturation is based on the empirical Linear Extrapolation Model (Greene & Pace, 1974). These are all common assumptions in protein folding, but may not apply to all proteins.

DATA & CODE AVAILABILITY

CheMelt can be used as an online app, Docker image, R shiny application, or Python package (*pychemelt*). The online tool can be accessed at https://spc.embl-hamburg.de/app/chemelt. The Docker image is available at https://hub.docker.com/r/emblspc/chemelt_espc. The R shiny application code is available at https://github.com/SPC-Facility-EMBL-Hamburg/thermochemicalDenaturationApp. The python package *pychemelt* code is available at https://github.com/osvalB/pychemelt. A Jupyter notebook with examples for simulating and fitting data are available at https://github.com/osvalB/pychemelt_analyses. All experimental data contained in the manuscript is available in FigShare (10.6084/m9.figshare.31889308).

ACKNOWLEDGEMENTS

This project has received funding from the European Union's Horizon 2020 research and innovation programme under the Marie Skłodowska-Curie grant agreement No 945405. The work is funded by a grant from the Danish National Research Foundation awarded to the Center for Proteins in Memory (PROMEMO) (DNRF133) and by an instrument supported by Carlsberg Foundation grant (CF21-0164) to M.K. at the Biophysics & Biochemistry Core Facility, Aarhus University, DK. Osvaldo Burastero is funded by the ARISE Fellowship (EMBL and the Marie Skłodowska-Curie Actions). Vili Lampinen and Francisca Pinheiro are funded by Lundbeckfonden (R483-2024-1763 & R449-2023-1396). We thank Kübra Fatima Eroglu for her help in preparing the GluN1 binder proteins, and Jeremias Widmann and Prof. Daniel Otzen for help in doing the circular dichroism measurements.

USAGE OF LARGE LANGUAGE MODELS

ChatGPT (https://chat.openai.com/) and Github Copilot (https://github.com/features/copilot) were used for coding assistance. The authors take full responsibility for the manuscript content and code.

SUPPORTING INFORMATION

The supplementary information contains eight figures, three tables and supplementary text describing the theory behind the fitting equations and practical instructions for use.

Link to Supplementary Information

CONFLICT OF INTEREST STATEMENT

The authors declare no conflicts of interest.

REFERENCES

Alexander, P., Fahnestock, S., Lee, T., Orban, J., & Bryan, P. (1992). Thermodynamic analysis of the folding of

the streptococcal protein G IgG-binding domains B1 and B2: why small proteins tend to have high denaturation temperatures. *Biochemistry*, *31*(14), 3597–3603.

Baldwin, R. L. (1986). Temperature dependence of the hydrophobic interaction in protein folding. *Proceedings of the National Academy of Sciences of the United States of America*, *83*(21), 8069–8072.

Burastero, O., Jones, N. C., Defelipe, L. A., Zavrtanik, U., Hadži, S., Hoffmann, S. V., & Garcia-Alai, M. M. (2025). ChiraKit: an online tool for the analysis of circular dichroism spectroscopy data. *Nucleic Acids Research*, *53*(W1), W158–W168.

Burastero, O., Niebling, S., Defelipe, L., Günther, C., Struve, A., & Garcia Alai, M. G. (2021). eSPC: an online data-analysis platform for molecular biophysics. *Acta Crystallographica. Section D, Structural Biology*, *77*(10), 1241–1250.

Cao, L., Coventry, B., Goreshnik, I., Huang, B., Sheffler, W., Park, J. S., … Baker, D. (2022). Design of protein-binding proteins from the target structure alone. *Nature*, *605*(7910), 551–560.

Dauparas, J., Anishchenko, I., Bennett, N., Bai, H., Ragotte, R. J., Milles, L. F., … Baker, D. (2022). Robust deep learning-based protein sequence design using ProteinMPNN. *Science (New York, N.Y.)*, *378*(6615), 49–56.

Greene, R. F., & Pace, C. N. (1974). Urea and guanidine hydrochloride denaturation of ribonuclease, lysozyme, α-chymotrypsin, and b-lactoglobulin. *Journal of Biological Chemistry*, *249*(17), 5388–5393.

Grene, I. K., Joachim, N., Pinheiro, F., Lampinen, V., Teilum, K., & Kjaergaard, M. (2025). Medium throughput protein expression and purification for protein design using heat lysis. *Protocols.io*. doi: 10.17504/protocols.io.dm6gpq6b5lzp/v1

Hamborg, L., Horsted, E. W., Johansson, K. E., Willemoës, M., Lindorff-Larsen, K., & Teilum, K. (2020). Global analysis of protein stability by temperature and chemical denaturation. *Analytical Biochemistry*, *605*, 113863.

Jaenicke, R., & Böhm, G. (1998). The stability of proteins in extreme environments. *Current Opinion in Structural Biology*, *8*(6), 738–748.

Jumper, J., Evans, R., Pritzel, A., Green, T., Figurnov, M., Ronneberger, O., … Hassabis, D. (2021). Highly accurate protein structure prediction with AlphaFold. *Nature*, *596*(7873), 583–589.

Koga, R., Yamamoto, M., Kosugi, T., Kobayashi, N., Sugiki, T., Fujiwara, T., & Koga, N. (2020). Robust folding of a de novo designed ideal protein even with most of the core mutated to valine. *Proceedings of the National Academy of Sciences of the United States of America*, *117*(49), 31149–31156.

Lindorff-Larsen, K., & Teilum, K. (2021). Linking thermodynamics and measurements of protein stability. *Protein Engineering, Design & Selection : PEDS*, *34*. doi: 10.1093/protein/gzab002

Magnusson, A. O., Szekrenyi, A., Joosten, H.-J., Finnigan, J., Charnock, S., & Fessner, W.-D. (2019). nanoDSF as screening tool for enzyme libraries and biotechnology development. *The FEBS Journal*, *286*(1), 184–204.

Marcos, E., Chidyausiku, T. M., McShan, A. C., Evangelidis, T., Nerli, S., Carter, L., … Baker, D. (2018). De novo design of a non-local β-sheet protein with high stability and accuracy. *Nature Structural & Molecular Biology*, *25*(11), 1028–1034.

Myers, J. K., Pace, C. N., & Scholtz, J. M. (1995). Denaturant m values and heat capacity changes: relation to changes in accessible surface areas of protein unfolding. *Protein Science : A Publication of the Protein Society*, *4*(10), 2138–2148.

Niebling, S., Burastero, O., Bürgi, J., Günther, C., Defelipe, L., Sander, S., … García-Alai, M. (2021). FoldAffinity: binding affinities from nDSF experiments. *Scientific Reports*, *11*(1), 9572.

Nojima, H., Ikai, A., Oshima, T., & Noda, H. (1977). Reversible thermal unfolding of thermostable phosphoglycerate kinase. Thermostability associated with mean zero enthalpy change. *Journal of Molecular Biology*, *116*(3), 429–442.

Pantoliano, M. W., Petrella, E. C., Kwasnoski, J. D., Lobanov, V. S., Myslik, J., Graf, E., … Salemme, F. R. (2001). High-density miniaturized thermal shift assays as a general strategy for drug discovery. *Journal of Biomolecular Screening*, *6*(6), 429–440.

Pezeshgi Modarres, H., Mofrad, M. R., & Sanati-Nezhad, A. (2016). Protein thermostability engineering. *RSC Advances*, *6*(116), 115252–115270.

Pinheiro, F., Nowak, J. S., Zueva, E., Pheasant, E. C., Grene, I. K., Lampinen, V., & Kjaergaard, M. (2025). Screening de novo designed protein binders in unpurified lysate using flow induced dispersion analysis. *Protein Science : A Publication of the Protein Society*, *34*(10), e70286.

Privalov, P. L. (1979). Stability of proteins: small globular proteins. *Advances in Protein Chemistry*, *33*, 167–241.

Razvi, A., & Scholtz, J. M. (2006). Lessons in stability from thermophilic proteins. *Protein Science : A*

Publication of the Protein Society, *15*(7), 1569–1578.
Rief, M., Gautel, M., Oesterhelt, F., Fernandez, J. M., & Gaub, H. E. (1997). Reversible unfolding of individual titin immunoglobulin domains by AFM. *Science (New York, N.Y.)*, *276*(5315), 1109–1112.
Sandeep Kumar, ‡., Chung-Jung Tsai, §. A., & Nussinov*§□, R. (2001). *Thermodynamic Differences among Homologous Thermophilic and Mesophilic Proteins†*. doi: 10.1021/bi0106383
Schrödinger, LLC. (2024). *The PyMOL Molecular Graphics System, Version 3.1.1*.
Seelig, J., & Schönfeld, H.-J. (2016). Thermal protein unfolding by differential scanning calorimetry and circular dichroism spectroscopy Two-state model versus sequential unfolding. *Quarterly Reviews of Biophysics*, *49*, e9.
Spolar, R. S., Livingstone, J. R., & Record, M. T., Jr. (1992). Use of liquid hydrocarbon and amide transfer data to estimate contributions to thermodynamic functions of protein folding from the removal of nonpolar and polar surface from water. *Biochemistry*, *31*(16), 3947–3955.
Teilum, K., Kragelund, B. B., & Poulsen, F. M. (2002). Transient structure formation in unfolded acyl-coenzyme A-binding protein observed by site-directed spin labelling. *Journal of Molecular Biology*, *324*(2), 349–357.
Teilum, K., Maki, K., Kragelund, B. B., Poulsen, F. M., & Roder, H. (2002). Early kinetic intermediate in the folding of acyl-CoA binding protein detected by fluorescence labeling and ultrarapid mixing. *Proceedings of the National Academy of Sciences of the United States of America*, *99*(15), 9807–9812.
Thomsen, J. K., Kragelund, B. B., Teilum, K., Knudsen, J., & Poulsen, F. M. (2002). Transient intermediary states with high and low folding probabilities in the apparent two-state folding equilibrium of ACBP at low pH. *Journal of Molecular Biology*, *318*(3), 805–814.
Vázquez Torres, S., Benard Valle, M., Mackessy, S. P., Menzies, S. K., Casewell, N. R., Ahmadi, S., … Baker, D. (2025). De novo designed proteins neutralize lethal snake venom toxins. *Nature*, *639*(8053), 225–231.
Vázquez Torres, S., Leung, P. J. Y., Venkatesh, P., Lutz, I. D., Hink, F., Huynh, H.-H., … Baker, D. (2024). De novo design of high-affinity binders of bioactive helical peptides. *Nature*, *626*(7998), 435–442.
Vermeer, A. W., & Norde, W. (2000). The thermal stability of immunoglobulin: unfolding and aggregation of a multi-domain protein. *Biophysical Journal*, *78*(1), 394–404.
Watson, J. L., Juergens, D., Bennett, N. R., Trippe, B. L., Yim, J., Eisenach, H. E., … Baker, D. (2023). De novo design of protein structure and function with RFdiffusion. *Nature*, *620*(7976), 1089–1100.
Zheng, B., Lu, Z., Wang, S., Liu, L., Ao, M., Zhou, Y., … Zheng, P. (2025). Computational design of superstable proteins through maximized hydrogen bonding. *Nature Chemistry*. doi: 10.1038/s41557-025-01998-3
Zhou, H.-X. (2002). Toward the physical basis of thermophilic proteins: linking of enriched polar interactions and reduced heat capacity of unfolding. *Biophysical Journal*, *83*(6), 3126–3133.
Žoldák, G., Jancura, D., & Sedlák, E. (2017). The fluorescence intensities ratio is not a reliable parameter for evaluation of protein unfolding transitions. *Protein Science : A Publication of the Protein Society*, *26*(6), 1236–1239.